REPRINTED FROM:

CHEMICAL PHYSICS

Chemical Physics 176 (1993) 97–108
North-Holland

Simulation of water solutions of Ni^{2+} at infinite dilution

M. Natália D.S. Cordeiro, Anna Ignaczak [1] and José A.N.F. Gomes
Departamento de Química, Faculdade de Ciências, Universidade do Porto, 4000 Porto, Portugal

Received 26 April 1993

NORTH-HOLLAND
AMSTERDAM – LONDON – NEW YORK – TOKYO

CHEMICAL PHYSICS

A journal devoted to experimental and theoretical research involving problems of both a chemical and a physical nature

Important: please adhere to instructions to authors, to be found on the last pages of each volume.

After acceptance of the paper for publication, further correspondence should be sent to the publishers (Drs. H.A. Arends, Editorial Department, Chemistry & Chemical Engineering Department, P.O. Box 330, 1000 AH Amsterdam, The Netherlands; FAX 31-20-5862459; telex 10704 espom nl; electronic mail X400: C=NL; A=400NET; P=SURF; O=ELSEVIER; S=VONK, I=W or RFC822: W. VONK@ELSEVIER.NL).

Chemical Physics is published semi-monthly. For 1993, 10 volumes, volumes 167-176 (30 issues altogether), have been announced. The subscription price for these volumes is Dfl. 4050.00 (US$ 2250.00). Postage and handling amount to Dfl. 330.00 (US$ 185.00). Therefore the total price is Dfl. 4380.00 (US$ 2435.00). The Dutch guilder price is definitive, dollar prices are for guidance only. Claims for issues not received should be made within six months of publication. If not, they cannot be honoured free of charge.

Subscriptions should be sent to the publisher: Elsevier Science Publishers B.V., Journals Department, P.O. Box 211, 1000 AE Amsterdam, The Netherlands, or to any subscription agent or bookseller.

US mailing notice. Chemical Physics (ISSN 0301-0104) is published semi-monthly by Elsevier Science Publishers (Molenwerf 1, P.O. Box 211, 1000 AE Amsterdam). Annual subscription price in the USA US$ 2435.00 (subject to change), including air speed delivery. Second class postage paid at Jamaica, NY 11431.
USA POSTMASTERS: Send address changes to: Chemical Physics, Publications Expediting, Inc., 200 Meacham Avenue, Elmont, NY 11003. Airfreight and mailing in the USA by Publication Expediting.

Printed in The Netherlands

Published semi-monthly

Chemical Physics 176 (1993) 97–108
North-Holland

Simulation of water solutions of Ni^{2+} at infinite dilution

M. Natália D.S. Cordeiro, Anna Ignaczak [1] and José A.N.F. Gomes
Departamento de Química, Faculdade de Ciências, Universidade do Porto, 4000 Porto, Portugal

Received 26 April 1993

A new ab initio pair potential is developed to describe the nickel–water interactions in Ni(II) aqueous solutions. Results of Monte Carlo simulations for the Ni(II)–$(H_2O)_{200}$ system are presented for this pair potential with and without three-body classical polarization terms (the water–water interaction is described by the ab initio MCY potential). The structure of the solution around Ni(II) is discussed in terms of radial distribution functions, coordination numbers and thermal ellipsoids. The results show that the three-body terms have a non-negligible effect on the simulated solution. In fact, the experimental coordination number of six is reproduced with the full potential while a higher value is predicted when the simple pairwise-additive potential is used. The equilibrium NiO distance for the first hydration shell is also dependent on the use of the three-body terms. Comparison of our distribution functions with those obtained by neutron-diffraction experiments shows a reasonable quantitative agreement. Statistical pattern recognition analysis has also been applied to our simulations in order to better understand the local thermal motion of the water molecules around the metal ion. In this way, thermal ellipsoids have been computed (and graphically displayed) for each atom of the water molecules belonging to the Ni(II) first hydration shell. This analysis revealed that the twisting and bending motions are greater than the radial motion, and that the hydrogens have a higher mobility than the oxygens. In addition, a thermodynamic perturbation method has been incorporated in our Monte Carlo procedure in order to compute the free energy of hydration for the Ni(II) ion. Agreement between these results and the experimental ones is also sufficiently reasonable to demonstrate the feasibility of this new potential for the nickel–water interactions.

1. Introduction

The study of aqueous solutions of transition metal ions is fundamental to understand a wide range of chemical processes in which these ions take part and on which, as it is well known, the solvent has a decisive role. In the past decades, our knowledge of the microscopic properties of these aqueous solutions has grown immensely due to the great improvements on experimental diffraction work [1] and theoretical simulations [2–15]. Among all transition metal ions, the Ni(II) ion has been extensively studied experimentally and good quality results exist.

The experimental studies of Ni^{2+} hydrated salts, based on neutron or X-ray scattering [16–18], showed a well resolved first hydration shell with six water molecules uniformly arranged around the central ion. This solvation structure was found to be remarkably insensitive to changes on the counterion, pressure or temperature. From a theoretical point of view, to our knowledge, only Bounds [3] carried out a molecular dynamics (MD) study of a Ni^{2+} solution using two-body potentials for the water–water and ion–water interactions. This author found a general agreement with the experimental results save for the high coordination number obtained. Bounds attributed this discrepancy to the two-body Ni^{2+}–water ab initio potential used in his simulations. There is an obvious need for new simulations for this ion using more reliable potentials for the nickel–water interactions and this is precisely the purpose of this work.

The outline of the paper is as follows. In the next section, several analytical potential functions for the Ni^{2+}–water two-body interactions are presented and examined. Details of the three-body ion–water–water classical polarization potential used are also given in that section. The actual two- and two- plus three-body model potentials chosen are then tested on Monte Carlo (MC) simulations of diluted Ni^{2+} aqueous solutions at $T = 298$ K. The results of these simulations

[1] Present address: Department of Theoretical Chemistry, University of Lódz, 90236 Lódz, Poland.

are collected in section 3 and compared, whenever possible, with recent neutron-diffraction data. Furthermore, a simple pattern recognition method is applied to our best simulation results. This method allows us to clarify the relative motion of the water molecules of the first solvation shell with respect to the central Ni(II) ion. The perturbation method used to calculate the free energy of hydration for this ion is also outlined and the results are used again to assess the quality of the proposed Ni^{2+}–water potential. Finally, the main results of this work are summarized in section 4.

2. Nickel–water interactions

2.1. Two-body ion–water potential

The potential surfaces used on the fits of the two-body Ni^{2+}–H_2O potentials were obtained from quantum ab initio calculations of the corresponding dimer. The ab initio calculations have been done at the UHF level using the GAUSSIAN 90 program [19]. The DZ basis set used for the water molecule was taken from the work of Dunning et al. [20] and for the Ni(II) ion (^{3}F ground state) the ECP/DZV basis set of Hay et al. [21] was used. More than 250 configurations of the Ni^{2+}–H_2O dimer were computed, keeping fixed the water molecule geometry (R_{OH}=0.957 Å and ∠HOH=104.5° [22]) and covering an important water configuration space around the ion [7]. From these calculations, the global energy minimum of −385.78 kJ/mol corresponding to a planar geometry of C_{2v} symmetry (R_{NiO}=1.96 Å) was found as expected. These results are quite similar to the all-electron results obtained by Bounds [3] using a high quality basis set (same geometry found with an energy of −368.0 kJ/mol at a NiO distance of 2.0 Å). It is also worth noting here that calculations made with another transition metal ion and using the same type of ECP/DZV basis set have shown that the basis set superposition errors are not very important for this type of basis sets [15]. The long distance behaviour of the calculations is also good, showing no unrealistic charge transfer [9–11].

The best choice of an analytical function to describe the interaction is always a delicate balance between a high quality fit to the data available and the simplicity that allows a fast computation. Moreover, certain conditions must be satisfied for the function to be physically acceptable when applied in the very short and in the long range. This type of concern is not relevant here as no long range correction is envisaged in the simulation and the short range behaviour will be checked in each case. Several analytical functions have been considered for the fit of the above set of ab initio computations. The first type of functions has an exponential part and was inspired on the work of Rode et al. [10] for the solvated zinc ion. The following two forms, V_1 and V_2, were then considered:

$$V_1 = \frac{q_i q_M}{R_{iM}} + \frac{A_{iM}}{R_{iM}^3} + \frac{B_{iM}}{R_{iM}^4} + C_{iM}\exp(-D_{iM}R_{iM}) + \sum_{j=1}^{2}\left(\frac{q_j q_M}{R_{jM}} + \frac{A_{jM}}{R_{jM}^3} + \frac{B_{jM}}{R_{jM}^4} + C_{jM}\exp(-D_{jM}R_{jM})\right), \quad (1)$$

where A_{iM}, A_{jM}, B_{iM}, B_{jM}, C_{iM}, D_{iM} and D_{jM} are the fitting parameters. R_{iM} and R_{jM} indicate, respectively, Ni(II)–oxygen and Ni(II)–hydrogen distances. q_i, q_j and q_M are the net atomic charges of the ith or jth atom of the water molecule and of Ni(II) taken from a Mulliken population analysis [23] of the isolated species. V_2 differs from V_1 only on the Coulombic terms, namely, the charge q_M of Ni(II) is not imposed but also considered as a fitting parameter:

$$V_2 = \frac{A_{iM}q_i}{R_{iM}} + \frac{B_{iM}}{R_{iM}^3} + \frac{C_{iM}}{R_{iM}^4} + D_{iM}\exp(-E_{iM}R_{iM}) + \sum_{j=1}^{2}\left(\frac{A_{jM}q_j}{R_{jM}} + \frac{B_{jM}}{R_{jM}^3} + \frac{C_{jM}}{R_{jM}^4} + D_{jM}\exp(-E_{jM}R_{jM})\right). \quad (2)$$

The second type of functions is a linear combination of R^{-n} terms and was taken from early works on other hydrated metalic ions [5,7,8,12,15]. The following two forms, V_3 and V_4, were used:

$$V_3 = A\left(\frac{q_i}{R_{iM}} + \sum_{j=1}^{2}\frac{q_j}{R_{jM}}\right) + B\left(\frac{1}{R_{iM}^2} - \frac{1}{2}\sum_{j=1}^{2}\frac{1}{R_{jM}^2}\right)$$
$$+ C\left(\frac{1}{R_{iM}^3} - \frac{1}{2}\sum_{j=1}^{2}\frac{1}{R_{jM}^3}\right) + \frac{D_{iM}}{R_{iM}^4} + \sum_{j=1}^{2}\frac{D_{jM}}{R_{jM}^4}$$
$$+ \frac{E_{iM}}{R_{iM}^5} + \sum_{j=1}^{2}\frac{E_{jM}}{R_{jM}^5} + \frac{F_{iM}}{R_{iM}^6} + \sum_{j=1}^{2}\frac{F_{jM}}{R_{jM}^6}$$
$$+ \frac{G_{iM}}{R_{iM}^{12}} + \sum_{j=1}^{2}\frac{G_{jM}}{R_{jM}^{12}}, \qquad (3)$$

where R_{iM}, R_{jM} again refer to the Ni(II)–oxygen and Ni(II)–hydrogen distances and q_i, q_j to the net atomic charges of the oxygen and hydrogen atoms of the water molecule (in this case, $q_O = -0.64$ au and $q_H = +0.32$ au). V_4 is similar to V_3 but for the absence of the R^{-n} terms with $n = 2, 3$:

$$V_4 = A\left(\frac{q_i}{R_{iM}} + \sum_{j=1}^{2}\frac{q_i}{R_{jM}}\right) + \frac{B_{iM}}{R_{iM}^4} + \sum_{j=1}^{2}\frac{B_{jM}}{R_{jM}^4}$$
$$+ \frac{C_{iM}}{R_{iM}^5} + \sum_{j=1}^{2}\frac{C_{jM}}{R_{jM}^5} + \frac{D_{iM}}{R_{iM}^6} + \sum_{j=1}^{2}\frac{D_{jM}}{R_{jM}^6}$$
$$+ \frac{E_{iM}}{R_{iM}^{12}} + \sum_{j=1}^{2}\frac{E_{jM}}{R_{jM}^{12}}. \qquad (4)$$

The fit of the above functions to the ab initio Ni^{2+}–H_2O energy points was made in the usual least-squares sense and a weighting function similar to that of ref. [24] was applied, namely

$$w_k = 1 + \Omega \exp[-(\Delta E_k - \Delta E_0)/kT], \qquad (5)$$

where ΔE_0 is the minimum interaction energy of the Ni(II)–H_2O system and the Ω parameter was fixed at 200. This was the best value found for Ω that, simultaneously, gave a greater importance to the attractive parts of the potential surface and did not deteriorate its repulsive parts.

A simple test of the fitted potentials is the comparison of their minima with those of the ab initio computations. Table 1 shows the resulting minima for all the model potentials together with the standard deviations obtained on their fittings. Potential V_4 was chosen as a compromise between the quality of the fit (smaller standard deviation and better proximity to the ab initio values) and the complexity of the analytical function. It should be noticed that the standard deviation achieved on the fit of this potential corresponds to only $\approx 4\%$ of the energy minimum.

Table 1
Comparison of minima for the most stable configuration of the Ni^{2+}–(H_2O) dimer obtained from ab initio calculations and from the model potentials. The standard deviations (σ) of the fits of the potentials are also shown

Model	ΔE_{min} (kJ/mol)	ΔR_{min} (Å)	σ (kJ/mol)
ab initio	−385.78	1.96	
V_1	−385.70	1.98	15.04
V_2	−385.75	1.98	14.93
V_3	−385.64	1.97	14.54
V_4	−385.85	1.98	14.61

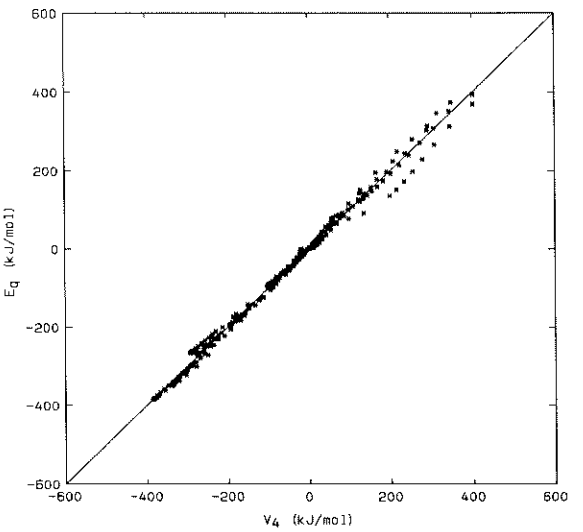

Fig. 1. Comparison between calculated interaction energies (E_q) and those resulting from the fitting to potential V_4.

The accuracy of the V_4 potential is also apparent in fig. 1, where all calculated ab initio interaction energies are plotted against those predicted by V_4. As one can see from this figure, the depicted points are very close to the ideal 45° line, particularly in the important attractive region. The full set of parameters of V_4 is given in table 2.

In all the following MC calculations, the V_4 potential has been used to describe the Ni(II)–water pair interactions. It should be noticed that this function has a unphysical short range behaviour. However, the energy barrier between the potential minimum and this unphysical attractive region is far too high to be of any concern during the simulations.

Table 2
Final parameters for the Ni^{2+}–H_2O ab initio pair potential function

Parameter	V_4 [a]
A	$+0.21631\times10^{1}$
B_{OM}	$+0.34325\times10^{2}$
B_{HM}	-0.17037×10^{2}
C_{OM}	-0.64110×10^{3}
C_{HM}	$+0.12383\times10^{3}$
D_{OM}	$+0.18746\times10^{4}$
D_{HM}	-0.20170×10^{3}
E_{OM}	-0.15557×10^{6}
E_{HM}	$+0.24888\times10^{4}$

[a] Energies in hartrees when bond distances are in bohrs.

2.2. Three-body ion–water–water polarization potential

A non-additive three-body Ni^{2+}–$(H_2O)_2$ correction may be added to the V_4 pair potential to improve the representation of the ion–water interaction energy. Following the work of Clementi et al. [25] this correction was modelled by a polarization energy, based on a classical water-bond polarizability model [26] of the form

$$P=-\sum_{b\in K}\sum_{\substack{i\in J\\ J\neq K}} q_i q_M[\alpha_b(\boldsymbol{R}_{Mb}\cdot\boldsymbol{R}_{ib}) + \delta_b(\boldsymbol{R}_{Mb}\cdot\boldsymbol{e}_b)(\boldsymbol{R}_{ib}\cdot\boldsymbol{e}_b)]/R_{ib}R_{Mb}^{5}, \quad (6)$$

where the first and the second summations extend over, respectively, the bonds of the water molecule K and the atoms of the water molecule J that should be different from K. The parameters and the variables of the above expression have the following meaning:

α_b: transverse polarizability of bond b in molecule K.

δ_b: anisotropy of bond b in molecule K.

q_i: charge of the ith atom of water molecule J.

q_M: charge of the metal ion.

$\boldsymbol{R}_{Mb}$: distance vector between the metal ion and the midpoint of the bond b in molecule K.

$\boldsymbol{R}_{ib}$: distance vector pointing from the ith atom of molecule J to the midpoint of the bond b of molecule K.

$\boldsymbol{e}_b$: unit vector in the direction of bond b.

Standard values [27] were attributed to the bond parameters above (i.e., $\alpha_b=3.91$ au and $\delta_b=1.42$ au) and the charges q_i used ($q_O=-0.64$ au and $q_H=+0.32$ au) have an associated dipole moment (1.85 D) similar to that of gaseous water [28]. The solute M (charge $q_M=2.0$ au) itself is not polarizable although it does contribute to the polarization $\boldsymbol{P}$.

3. Monte Carlo simulations

The MC simulations have been carried out on the NVT ensemble at a temperature of 298 K for a diluted solution of Ni(II), represented by the system Ni^{2+}–$(H_2O)_{200}$. In these simulations, a cubic box of side lengths of about 18 Å has been chosen in order to get a density of ≈ 1 g/cm^3 for the 200 water molecules. Periodic boundary conditions under the minimal image convention [29] have been considered. The simulations have been done according to the Metropolis algorithm [30] and the number of configurations used for statistical equilibration and sampling was 2×10^6. Several water–water potentials are currently used in simulation. In this work, the MCY potential [31] was chosen as it is the more extensively tested non-empirical water–water potential. To describe the ion-water interactions, the V_4 potential or this potential with inclusion of the ion–water–water polarization terms (V_4+P) have been used.

3.1. The structure

3.1.1. Radial distribution functions and coordination numbers

The structure of the solution around the Ni^{2+} will be discussed in terms of radial distribution functions (RDF) and running coordination numbers [n_O, n_H]. The main results of the MC simulations for the Ni^{2+}–$(H_2O)_{200}$ system using the V_4 pair potential with and without the three-body potential are given in table 3 and in fig. 2. In figs. 2a and 2b two sharp peaks can be observed, one for the RDF_{NiO} and the other for the RDF_{NiH}, this one shifted to larger distances relatively to the former one. These two peaks are clearly related to the first hydration shell of the nickel ion. The displacement to larger distances observed for the first peak of the RDF_{NiH} means that, in this region, the water molecules are well oriented to obey the dominant ion–water interactions with their oxygen atoms pointing to the Ni(II). The first peaks of the

Table 3
Nickel(II)–water coordination. The experimental results are from a 2.0 molal solution of $NiCl_2$ [18] and the MD results are from a simulation at 316 K of the Ni^{2+}–$(H_2O)_{64}$ system using pair potentials [3]

	Experimental	Simulated		
		this work (MC)		MD
		V_4	V_4+P	
1st shell				
R_{NiO} (Å) [a]	2.07	2.09	2.07	2.17
R_{NiH} (Å) [a]	2.69	2.75	2.69	2.76
n_O [b]	6.0	8.00	6.00	8.00
n_H [b]	11.8	16.24	12.04	
2nd shell				
n_O [c]	18±2	17.95	16.27	
n_H [c]	36±4	43.68	38.45	

[a] Position of the maxima on the first peaks of the radial ion–oxygen (R_{NiO}) and ion–hydrogen (R_{NiH}) distribution functions.
[b] Calculated by integrating the radial ion–oxygen distribution function (n_O) or the radial ion–hydrogen distribution function (n_H) up to their first peak minima.
[c] Calculated by integrating the radial ion–oxygen distribution function (n_O) or the radial ion–hydrogen distribution function (n_H) between their first and second peak minima.

RDF_{NiO} and RDF_{NiH} of fig. 2a appear, respectively, at 2.09 and 2.75 Å and do overlap to some extent. The corresponding peaks for the simulation with the V_4+P potential appear at shorter distances than the above ones (see fig. 2b and table 3). In this case, the RDF_{NiO} is equal to zero in the zone 2.30 Å$< R_{NiO} <$ 3.30 Å, which is precisely the zone where the first peak of the RDF_{NiH} appears. Such behaviour of the RDF of the V_4+P simulation suggests that the first hydration shell is much better defined and has a more rigid structure than the one obtained on the V_4 simulation. From figs. 2a and 2b one can also notice the existence of a second shell for $R_{NiO} > 3$ Å, clearly much less structured than the first one. However, the existence of a second shell is only detected on the V_4+P coordination number plots, as the V_4 curves outside the first shell have a very flat behaviour without any major deviations.

As seen in table 3, the results obtained for the V_4+P simulation are in excellent agreement with the experimental values, while the V_4 simulation gives an overestimation for all values, in particular, the Ni^{2+} first coordination number. The same overestimation is obtained by Bounds on his MD simulations (see table 3) with pairwise additive potentials. It should be also noticed that the number of oxygens and hydrogens computed for the second hydration shell on the V_4+P simulation are reasonably similar to those suggested by Powell et al. [18]. However, it should

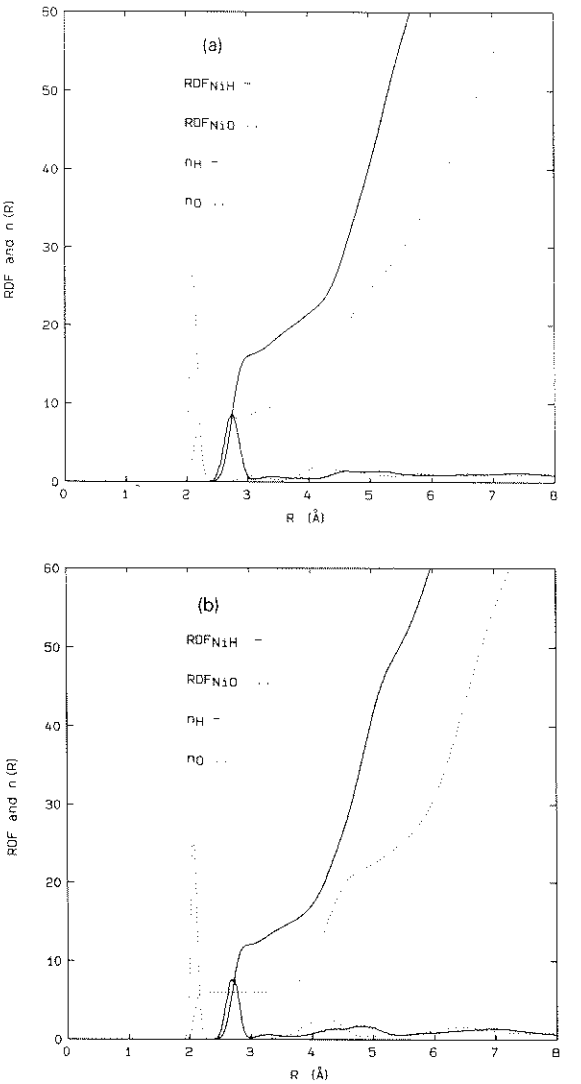

Fig. 2. Ion–hydrogen (RDF_{NiH}) and ion–oxygen (RDF_{NiO}) radial distribution functions and their respective running coordination numbers (n_H and n_O) for the simulation of a diluted Ni^{2+} solution at 298 K, using (a) the V_4 potential and (b) the V_4+P potential.

be stressed that neither the experimental nor our results for these values are very precise.

3.1.2. Comparison with neutron-diffraction data

Neutron-diffraction methods in conjunction with isotopic substitution are nowadays powerfull techniques capable of yielding unambiguous and detailed information on the structure of aqueous ionic solutions.

Powell et al. [18] have recently measured the first-order difference neutron functions $\Delta_{Ni}(K)$ (difference spectrum function of two solutions that only differ on the nickel isotopic composition) for 2.0 molal solutions of $NiCl_2$ in light and heavy water. By Fourier transforming the $\Delta_{Ni}(K)$ functions they obtain real-space difference functions $G_{Ni}(R)$, that are linear combinations of all partial RDF involved. Explicity,

$$G_{Ni}(R) = A(RDF_{NiO} - 1) + B(RDF_{NiD} - 1) + C(RDF_{NiH} - 1) + D(RDF_{NiCl} - 1) + E(RD_{NiNi} - 1)\,, \quad (7)$$

where A, B, C, D and E are weighting factors determined by the scattering lengths and concentrations of the several atoms in the measured solution. Normally, the D and E factors are much smaller than the A, B and C factors and thus $G_{Ni}(R)$ directly provides the characteristics of the ion coordination in solution. Based on the assumption that the partial structure factors $S_{NiO}(K)$ and $S_{NiH}(K)$ are the same in H_2O and D_2O, Powell et al. have computed the partial structure factor $S_{NiH}(K)$ by combining the two $\Delta_{Ni}(K)$ for the solutions in H_2O and D_2O. The Fourier transform of $S_{NiH}(K)$ gives the partial $RDF_{NiH}(R)$. The results of the simulations may be compared with these experimental results as shown in fig. 3 for our best simulation results (using the V_4+P ion–water potential). The data in this figure show that the two RDF_{NiH} agree in their general features, although the height of the experimental peaks is clearly much smaller than the calculated one and their width much larger. This is, probably, the consequence of a defect of the ion–water potential used which may still be too deep. However, it should be recalled that the experimental solutions were measured at 2.0 molal solutions while the present MC work refers to an infinite dilute solution. On the other hand, earlier experiments with Ni(II) solutions [17] have shown that the widths of the first RDF peaks tend to decrease with an increase of the concentration although their position do not vary with the concentration. This

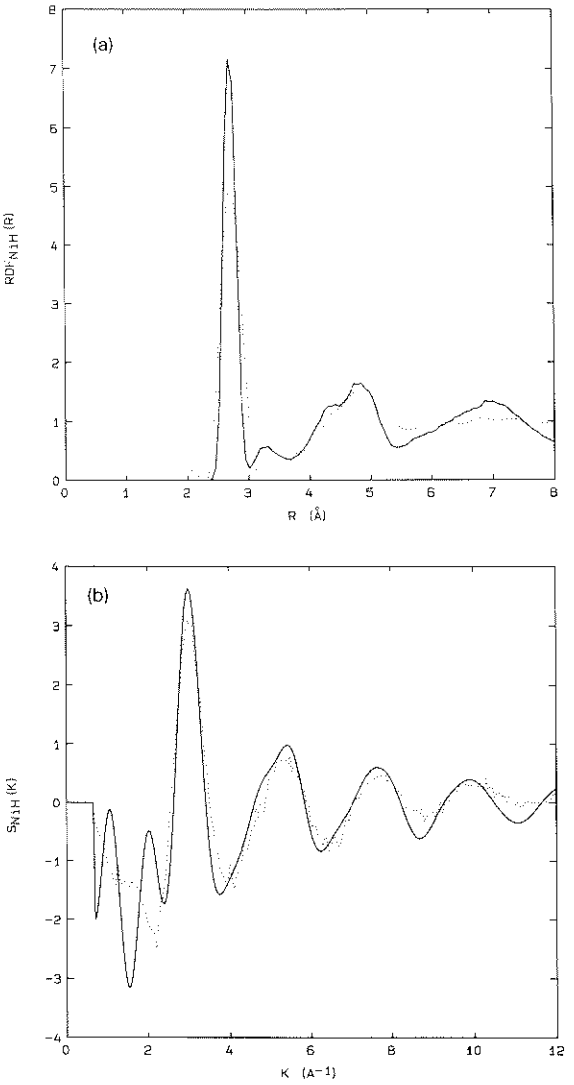

Fig. 3. (a) Partial radial distribution function RDF_{NiH} for Ni(II). Full curve: Monte Carlo results using the V_4+P and MCY potentials. Dotted curve: Experimental results of Powell et al. [18] for a 2.0 molal solution of $NiCl_2$ (to avoid confusion in the graph, the unphysical oscillations of the experimental curve below $R = 1.8$ Å are not displayed). (b) Partial structure function S_{NiH} for Ni(II). Full curve: Monte Carlo results using the V_4+P and MCY potentials. Dotted curve: Experimental results of Powell et al. [18] for a 2.0 molal solution of $NiCl_2$.

means that the strong octahedral coordination around the Ni(II) is expected to be less perturbed for lower concentrations, just as shown in fig. 3a. The agreement between the calculated $S_{NiH}(K)$ and the experimental one is also satisfactory (see fig. 3b), particularly in what concerns the position and value of the first maxima. A discrepancy is found at low K for the $S_{NiH}(K)$ (fig. 3b) and at high R ($R>6$ Å) for the $RDF_{NiH}(R)$ (fig. 3a). This may be an artifact of the finite size of the cubic box used in the simulation. On the other hand, there may be room for improvement of the V_4+P ion–water interactions, at least, in the longer range. In fact, this is not surprising since our MC simulations use a Coulombic truncated potential and long-range electrostatic interactions are not explicitly taken in account (for instance, by using a Ewald sum [32]). However, the present comparisons show that the overall description of the interactions in adequate in our model.

3.1.3. Water motion of the first Ni(II) shell

In order to estimate the geometrical disposition of the water molecules in the first shell, a microscopical pattern recognition analysis of the significant structures of the Ni(II) solution for the V_4+P simulation has been done using a technique similar to that developed by Tapia and Lluch [33]. First, the equilibrium configuration space was sorted so that all water molecules outside the first hydration shell were discarded (a cutoff radius $R_{NiO}=2.2$ Å was used). Then, the configurations were divided into classes through a geometrical criteria based on the oxygen–oxygen interconfiguration distances (see ref. [5] for details on this classification).

In this work, the above technique has been extended to also include the hydrogen atoms. The configuration space of the hydrogen atoms of each one of the six water molecules was scanned in the two relevant angles, namely, the angle between the water C_{2v} axis and the local radial direction axis and the angle of rotation of the hydrogen atoms measured in relation to the water C_{2v} axis. the classes were defined by a 30° interval in these two angles for each of the six water molecules. It was found that about 60% of the configurations analysed belong to a single class as defined above by the criterium on the oxygen and hydrogen atoms.

Each final class may be seen as a sampling of the thermal fluctuations around the preferred conformation of the solvation shell. Therefore, each of these classes is a distribution that can be considered as a trivariate normal distribution of the translation random variables X, Y, Z [4]. As usual, the probability density function $f(X, Y, Z)$ of the three joint variables can be used to find the probability, $P(S)$, that a point $[X, Y, Z]$ (in this case, the coordinates of a water molecule) falls in the region S by integration:

$$P(S)=\int\int\int_{S} f(X, Y, Z)\,\mathrm{d}X\,\mathrm{d}Y\,\mathrm{d}Z\,, \tag{8}$$

where $f(X, Y, Z)$ should be normalized.

This density function, which can be designated as $f(\boldsymbol{R})$ in vector notation, has the following form:

$$f(\boldsymbol{R})=\frac{[\det(\mathbf{M}^{-1})]^{1/2}}{(3\pi)^{3/2}} \times\exp[-\tfrac{1}{2}(\boldsymbol{R}-\langle\boldsymbol{R}\rangle)^{\mathrm{T}}\mathbf{M}^{-1}(\boldsymbol{R}-\langle\boldsymbol{R}\rangle)]\,, \tag{9}$$

where $\mathbf{M}^{-1}$ is the inverse of the variance–covariance matrix $\mathbf{M}$, $\langle\boldsymbol{R}\rangle$ means the average of the random variable $\boldsymbol{R}$ and the superscript T means transpose of. The matrix $\mathbf{M}$ is well known [34] and contains the variances and covariances of the random variables X, Y and Z. This matrix is obviously dependent on the temperature as it reflects the mobility of any particular atom. Diagonalization of the matrix $\mathbf{M}$ gives the principal axes of the ellipsoids, the so-called thermal ellipsoids [35], of the form

$$f(Y_1, Y_2, Y_3)=\frac{(\sigma_1\sigma_2\sigma_3)^{-1}}{(2\pi)^{3/2}} \times\exp[-\tfrac{1}{2}(Y_1^2/\sigma_1^2+Y_2^2/\sigma_2^2+Y_3^2/\sigma_3^2)]\,, \tag{10}$$

where Y_1, Y_2 and Y_3 are the principal axes of the thermal ellipsoids and σ_1^2, σ_2^2 and σ_3^2 are the variances along those principal axes. The ellipsoids of eq. (10) can be displayed graphically and represent the thermal motion of each atom of the water molecules.

In our case, the matrix $\mathbf{M}$ was only computed for the most populated class of configurations found by the technique described above. Table 4 gives the variances σ_1^2, σ_2^2 and σ_3^2 for the atoms falling inside the Ni(II) first shell, the six hexacoordinated oxygens and the corresponding twelve hydrogens. The values in this table show that the motion of the hydrogen atoms is larger (approximately by a factor of 2) than

Table 4
Amplitudes of motion (Å^2) of each atom on the first hydration shell of Ni(II)

Atom	σ_1^2	σ_2^2	σ_3^2
O_1	0.042	0.026	0.003
O_2	0.030	0.024	0.002
O_3	0.068	0.035	0.003
O_4	0.036	0.019	0.003
O_5	0.039	0.019	0.003
O_6	0.058	0.023	0.003
H_1	0.068	0.039	0.005
H_2	0.047	0.037	0.004
H_3	0.096	0.044	0.005
H_4	0.046	0.027	0.006
H_5	0.059	0.035	0.006
H_6	0.110	0.033	0.006
H_7	0.068	0.042	0.005
H_8	0.046	0.028	0.006
H_9	0.101	0.051	0.006
H_{10}	0.048	0.036	0.006
H_{11}	0.062	0.029	0.005
H_{12}	0.100	0.035	0.006

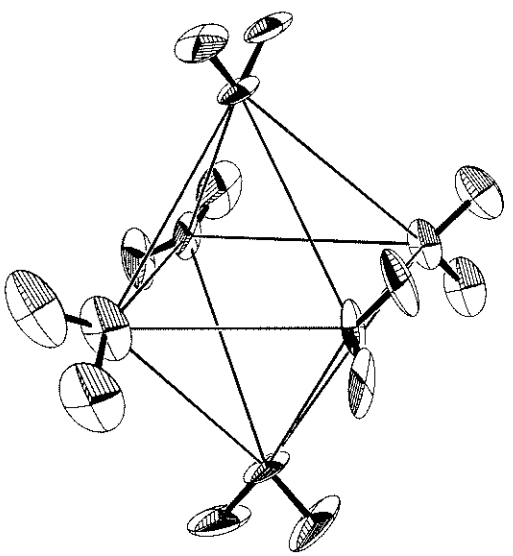

Fig. 4. Stereo plot of thermal ellipsoids for each atom in the first shell of the aqueous infinite diluted solution of Ni(II).

that of the oxygen atoms. On the other hand, for each atom there is always a direction of motion which is smaller than the other two. This can be identified with the radial motion by looking at the resulting stereo plot of the atom's thermal ellipsoids in fig. 4, as produced by the ORTEP program [36]. Bending and twisting motions seem to be preferred to the radial motion as indicated by the form of the ellipsoids of fig. 4. On the other hand, the large variations on the sizes of the hydrogen ellipsoids probably reflect the looser nature of the second shell of the Ni(II) ion.

3.2. The thermodynamics

Table 5 reports the average interaction energies per water molecule for the MC simulations of the Ni^{2+}–$(H_2O)_{200}$ system, using the V_4 pair potential and the V_4+P polarization potential. By comparing the results of this table, it can be seen that the inclusion of the polarization causes a decrease on the total energy, resulting not only from the repulsive contribution of the three-body polarization energy but also from the observed decrease on the ion–water two-body energy. The contribution of the water–water binding energy to the total energy of ionic solution is, however, more stabilizing in the V_4+P simulation than in the V_4 simulation. Essentially the same energetic trends have been observed for similar MC simulations of another transition metal ion [15].

In table 5, the hydration enthalpies (ΔH_{hydr}), estimated by subtracting the total interaction energies of the ionic solutions from that of pure water, are shown for the two potentials. Comparison with the experimental measured enthalpy of Ni(II) shows that the estimated enthalpies are too exotermic although less in the case of the V_4+P potential. Notice that these are rough estimates of the hydration enthalpy and thus the comparisons with the experimental data only allows a rough evaluation of the energetic performance of the potentials. However, they certainly show that even the best result, that for V_4+P, overestimates the energy data for this ion.

To better assess the energetic performance of the V_4+P potential, a thermodynamic perturbation simulation has been carried out to compute the Helmholtz free-energy of hydration of the Ni(II) ion. To compute this free-energy, the following process, that corresponds to the conversion of one water molecule of liquid water to Ni(II) ion, was simulated [37]:

$$H_2O(N, \text{aq.}) \leftrightarrow H_2O(N-1, \text{aq.}) + Ni^{2+}(\text{aq.}) , \quad (11)$$

where $H_2O(N, \text{aq.})$ means liquid water and, in this

Table 5
Thermodynamic results (in kJ/mol) of Ni(II) in water at 298 K

Method	ΔE_{ss} [a]	ΔE_{sx} [b]	ΔE_{tot} [c]	ΔH_{hydr}	ΔG_{hydr}
theor. MC (this work)					
V_4	−30.13	−24.02	−54.16	−3406 [d]	
V_4+P	−33.72	−19.06	−51.30 (1.479)	−2833 [d]	−2583 [e]
exp. [f]				−2171	−2068

[a] Energy per water molecule for the total two-body water–water interactions.
[b] Energy per water molecule for the total two-body ion–water interactions.
[c] Energy per water molecule for the total interactions. In the case of the V_4+P simulation, the total three-body interaction energy is also given in parentheses.
[d] Computed as $\Delta H_{hydr}=\Delta E_{tot}(Ni^{2+}-(H_2O)_{200})-\Delta E_{tot}((H_2O)_{200})$.
[e] MC value refers to the Helmholtz free energy of hydration ΔA_{hydr}.
[f] Ref. [38].

case, N was fixed at 125. Eq. (11) is a simple process of simulating the real hydration process, this is

$$H_2O(g.)+Ni^{2+}(g.)\leftrightarrow Ni^{2+}(aq.)\,. \tag{12}$$

However, the differences between processes (11) and (12) are expected to be negligible (of the order of 1 kJ/mol [37]) when compared with the value of the free energy of the Ni(II) ion (>-2000 kJ/mol [38]).

A coupling parameter, λ, that slowly converts the reference system ($\lambda=0$) into the perturbed system ($\lambda=1$) was incorporated on the simulation by considering an hybrid interaction potential of the form

$$U_{pot}(\lambda)=(1-\lambda)U_{ref}+\lambda U_{pert}\,, \tag{13}$$

where U_{ref} refers to the potential energy of the reference system, the $H_2O(N,$ liq.) system, and U_{pert} to the potential energy of the perturbed system, the $Ni^{2+}-(H_2O)_{N-1}$(aq.) system.

The free energy of hydration, ΔA_{hydr}, is then computed as [39]

$$\Delta A_{hydr}=-kT\sum_{w=0}^{N-1}\ln\langle\exp\{-[U_{pot}(\lambda_{w+1})-U_{pot}(\lambda_w)]/kT\}\rangle_{\lambda_w}\,. \tag{14}$$

where $\langle\ \rangle_{\lambda_w}$ means a canonical average over the intermediate system $U_{pot}(\lambda_w)$ as a reference system and N is the total number of windows.

To smoothly transform the reference system into the perturbed one, λ has been incremented through the formula [37]:

$$\lambda_{w+1}=\tfrac{1}{2}\{1+\tanh[(-N/2+w)W_0)]\}\,,\quad w=0,N-1\,, \tag{15}$$

where a value of 0.02 was given to the constant W_0. This value ensures that the changes in free energy were very small on the first and last windows.

Although a better estimate of the statistical errors and of the hysteresis could have been found with independent forward ($\lambda=0\rightarrow\lambda=1$) and backward ($\lambda=1\rightarrow\lambda=0$) simulations, only the forward simulation was performed. However, this forward simulation was done with double-wide sampling [40] to obtain simultaneously the free-energy changes for $\lambda_w\rightarrow\lambda_{w+1}$ and $\lambda_w\rightarrow\lambda_{w-1}$. The value of the free energy reported below is thus an average of the forward and backward results obtained in the single simulation of process (11). This simulation started with an equilibrated sample of 125 water molecules and the total number of windows used was $N=4000$. In each window, C (≈ 5000) configurations were generated and the free-energy changes were computed by averaging over the last $C/2$ generated configurations.

Table 5 presents the resulting ΔA_{hydr} of the Ni(II) ion, to be compared with the experimental data available, namely the Gibbs free energy of hydration, ΔG_{hydr}, of this ion. Notice that the differences between ΔG and ΔA are negligible in relation to the quantity computed. In fact, to the best of our knowledge, free-energy changes of this magnitude have never been calculated. As can be seen in this table, and as partially expected from the above estimates of

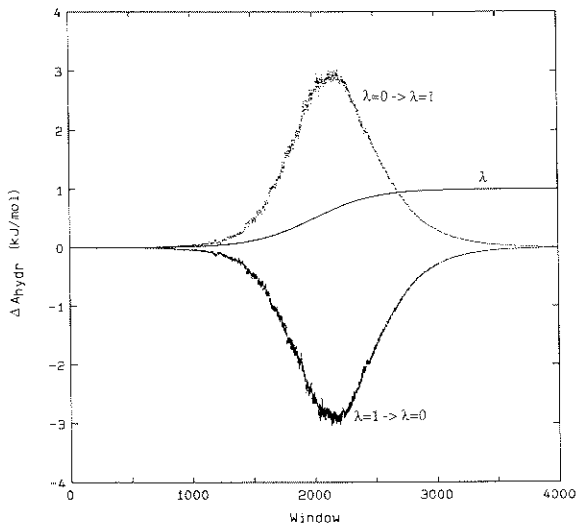

Fig. 5. Variation of ΔA_{hydr} of the Ni(II) ion in each window. Full curve: Variation of λ. Dotted curve: forward direction ($\lambda=0\rightarrow\lambda=1$). Broken curve: reverse direction ($\lambda=1\rightarrow\lambda=0$).

ΔH_{hydr}, the ΔA_{hydr} value obtained is overestimated with respect to the experimental one. The use of a larger sample, more windows and a larger number of generated configurations for each window will certainly improve the agreement with the experimental data. On the other hand, a more proper account for the hysteresis and of other statistical errors would also have be obtained if the forward and backward simulations were ran independently. However, the present single simulation presents an acceptable hysteresis as can be noticed on fig. 5, where the variation of ΔA_{hydr} in each window is plotted for the two directions $\lambda=0\rightarrow\lambda=1$ and $\lambda=1\rightarrow\lambda=0$.

Nevertheless, the principal reason for the disagreement should lie on the ion–water potential model used on the simulation. In fact, our potential model leaves out some important non-additive terms, i.e., the short-range exchange ion–water–water terms. Consideration of those terms, as also noted before for the solvated Cu(II) ion [15] and other ions [41], would probably improve the value ΔA_{hydr}.

4. Conclusions

In this paper, MC simulations are presented for a diluted aqueous solution of Ni(II), using a new ab initio pair potential with and without three-body classical polarization terms. Marked changes on the hydration number (n) and on the optimal NiO distances (R_{NiO}) of this ion's first shell are obtained when the pair potential alone is used ($n=8$, $R_{NiO}=2.09$ Å) or when it is supplemented with the polarization terms ($n=6$, $R_{NiO}=2.07$ Å). It should be remembered that another simulation study of Ni^{2+} [3], based on a two-body ab initio Ni^{2+}–H_2O potential, did also give a coordination number of eight for the first shell. This author suggested that it was quite possible that the problem lied on the ion–water potential used, which is certainly confirmed by the present results. This suggests that the ab initio pair potentials, save for a few exceptions [4,8,12,13], seem to be strongly inadequate to describe the interactions between transition metal ions and water. Pair potentials of hydrated ions different from the last class were also shown to be quite inappropriate and their refinement with polarization terms seems to correct them properly [41,42].

Overall, the agreement between a recent neutron diffraction study and the present MC simulations with the polarization potential (the V_4+P potential), as shown above in section 3, suggests that the intermolecular configurations obtained on its simulation reproduce sufficiently well the real Ni(II) hydrated system. On the other hand, a simple pattern recognition method applied to our best simulation results allowed us to dissect the water motion around the ion on its first shell. This shows that most of the water motion is due to the hydrogen atoms and that the Ni(II)–water radial motion is minimal. This seems to be a definitive feature of strongly hydrated ions as similar results were found for other solvated ions [4].

It should be said however, that further improvements on the present Ni(II)–water potential are needed, judging from the attained thermodynamic results. As already mentioned, this potential still lacks the short range contributions of the non-additive ion–water–water exchange terms and their inclusion is expected to correct it on the right way. A better description of the electrostatic interactions at long range is also likely to improve the present results. On the other hand, there is an obvious need for new simulation studies of this ion at higher concentrations and with counterions in order to make the comparisons

with the experimental work more reliable. Studies on these and other related questions are now in progress in our laboratory.

Acknowledgement

Financial support from JNICT (Lisbon) is acknowledged. The work of AI in Porto was made possible by a leave of absence from the University of Lòdz (Poland) and a research fellowship from the University of Oporto. We thank Dr. H. Powell for helpful discussions and for supplying us with the neutron-diffraction data in tabular form, Dr. P. Matias for his help with the ORTEP program, and our colleague Alexandre L. Magalhães for his interest in this work and his invaluable suggestions.

References

[1] A.K. Soper, G.W. Neilson, J.E. Enderby and R. Howe, J. Phys. C 10 (1977) 1793;
J.E. Enderby and G.W. Neilson, Rept. Prog. Phys. 44 (1981) 593;
M. Magini, G. Licheri, G. Piccaluga, G. Paschina and G. Pinna, X-ray diffraction of ions in aqueous solutions: hydration and complex formation (CRC Press, Boca Raton, 1988);
G.W. Neilson, Z. Naturforsch. 46a (1991) 100.
[2] E. Clementi, G. Corongiu, B. Jönsson and S. Romano, J. Chem. Phys. 72 (1980) 260.
[3] D.G. Bounds, Mol. Phys. 54 (1985) 1335.
[4] F.T. Marchese and D.L. Beveridge, Intern. J. Quantum Chem. 29 (1986) 619.
[5] A.G. Lafont, J.M. Lluch, A. Oliva and J. Bertrán, Chem. Phys. 111 (1987) 241.
[6] L.A. Curtiss, J.W. Halley, J. Hautman and A. Rahman, J. Chem. Phys. 86 (1987) 2319.
[7] M.N.D.S. Cordeiro, J.A.N.F. Gomes, A.G.-Lafont, J.M. Lluch, A. Oliva and J. Bertrán, J. Chem. Soc. Faraday Trans. II 84 (1988) 693.
[8] A.G.-Lafont, J.M. Lluch, A. Oliva and J. Bertrán, J. Comput. Chem. 9 (1988) 819.
[9] C.L. Kneifel, H.L. Friedman and M.D. Newton, Z. Naturforsch. 44a (1989) 385.
[10] Y.P. Yongyai, S. Kokpol and B.M. Rode, Chem. Phys. 156 (1991) 403.
[11] B.M. Rode and S.M. Islam, J. Chem. Soc. Faraday Trans. II 88 (1992) 417.
[12] M.N.D.S. Cordeiro, R. Cammi, J.A.N.F. Gomes and J. Tomasi, Theoret. Chim. Acta 82 (1992) 165.
[13] L. Curtiss, J.W. Halley and X.R. Wang, Phys. Rev. Letters 69 (1992) 2435.
[14] F. Floris, M. Persico, A. Tani and J. Tomasi, Chem. Phys. Letters 199 (1992) 518.
[15] M.N.D.S. Cordeiro and J.A.N.F. Gomes, J. Comput. Chem. 14 (1993) 629.
[16] H. Ohtaki, T. Yamaguchi and M. Maeda, Bull. Chem. Soc. Japan 49 (1976) 701.
[17] J.R. Newsome, G.W. Neilson, J.E. Enderby and M. Sandstrom, Chem. Phys. Letters 82 (1981) 399;
N.A. Hewish, G.W. Neilson and J.E. Enderby, Nature 297 (1982) 138;
G.W. Neilson and J.E. Enderby, Proc. Roy. Soc. A 390 (1983) 353.
[18] D.H. Powell, G.W. Neilson and J.E. Enderby, J. Phys. Condens. Matter 1 (1989) 8721.
[19] M.J. Frisch, M. Head-Gordon, G.W. Trucks, J.B. Foresman, H.B. Schlegel, K. Raghavachari, M.A. Robb, J.S. Binkley, C. Gonzalez, D.J. Defrees, D.J. Fox, R.A. Whiteside, R. Seeger, C.F. Melius, J. Baker, R.L. Martin, L.R. Kahn, J.J.P. Stewart, S. Topiol and J.A. Pople, GAUSSIAN 90 (Gaussian, Inc., Pittsburgh, PA, 1990).
[20] T.H. Dunning and P.J. Hay, Methods of electronic structure theory (Plenum Press, New York, 1976).
[21] P.J. Hay and W.R. Wadt, J. Chem. Phys. 82 (1985) 270.
[22] W.S. Benedict, N. Gailar and E.K. Plyler, J. Chem. Phys. 24 (1956) 1139.
[23] R.S. Mulliken, J. Chem. Phys. 23 (1955) 1833, 1841, 2338, 2343.
[24] S. Swaminathan, R.J. Whitehead, E. Guth and D. Beveridge, J. Am. Chem. Soc. 99 (1977) 7817.
[25] E. Clementi, H. Kistenmacher, W. Kolos and S. Romano, Theoret. Chim. Acta 55 (1980) 257;
G. Corongiu, M. Migliore and E. Clementi, J. Chem. Phys. 90 (1989) 4629.
[26] P. Claverie, Intermolecular interactions from diatomics to biopolymers, ed. B. Pullman (Wiley, New York, 1978) pp. 71–305.
[27] J.O. Hirschfelder, C.F. Curtiss and R.B. Bird, Molecular theory of gases and liquids (Wiley, New York, 1954).
[28] D. Eisenberg and W. Kauzmann, The structure and properties of water (Oxford Univ. Press, New York, 1969).
[29] M.P. Allen and D.J. Tildesley, Computer simulation of liquids (Oxford Univ. Press, Oxford, 1987).
[30] N. Metropolis, A.W. Rosenbluth, A.H. Teller and E. Teller, J. Chem. Phys. 21 (1953) 1087.
[31] O. Matsuoka, E. Clementi and M. Yoshimine, J. Chem. Phys. 64 (1976) 1351.
[32] P.P. Ewald, Ann. Physik (Leipzig) 64 (1921) 253.
[33] O. Tapia and J.M. Lluch, J. Chem. Phys. 83 (1985) 3970.
[34] K.S. Miller, Multidimensional Gaussian distributions (Wiley, New York, 1964);
E. Prince, Mathematical techniques in crystallography and material science (Springer, New York, 1982).
[35] J.D. Dunitz, X-ray and the structure of organic molecules (Cornell University Press, Ithaca, 1979).

[36] C.K. Johnson, ORTEP-II: a Fortran thermal ellipsoid plot program for crystal structure illustrations, ORNL-5138, Oak Ridge National Laboratory, Tennessee (1976).
[37] M. Migliore, G. Corongiu, E. Clementi and G.C. Lie, J. Chem. Phys. 88 (1988) 7766.
[38] K.L. Friedman and C.V. Krishnan, Thermodynamics of ion hydration, in: Water: a comprehensive treatise, Vol. 3, ed. F. Franks (Plenum Press, New York, 1973).
[39] R.W. Zwanzig, J. Chem. Phys. 22 (1954) 1420;
D.A. McQuarrie, Statistical mechanics (Harper and Row, New York, 1976).
[40] W.L. Jorgensen and C. Ravimohan, J. Chem. Phys. 83 (1985) 3050.
[41] T.P. Lybrand and P.A. Kollman, J. Chem. Phys. 83 (1985) 292;
P. Cieplak, T.P. Lybrand and P.A. Kollman, J. Chem. Phys. 86 (1987) 2867;
P. Cieplak and P.A. Kollman, J. Chem. Phys. 92 (1990) 6761;
L.X. Dang, J.E. Rice, J. Caldwell and P.A. Kollman, J. Am. Chem. Soc. 113 (1991) 2481.
[42] M. Sprik and M.L. Klein, J. Chem. Phys. 89 (1988) 7556;
M. Sprik, J. Phys. Chem. 95 (1991) 2283.